

Construction of occipital bone fracture using B-spline curves

Abdul Majeed 1 · Abd Rahni Mt Piah 2 · Zainor Ridzuan Yahya 3 · Johari Yap Abdullah 4 · Muhammad Rafique 5

Received: 29 June 2017 / Accepted: 10 July 2017

© SBMAC - Sociedade Brasileira de Matemática Aplicada e Computacional 2017

Abstract Treating trauma to the cranio-maxillofacial region is a great challenge and requires expert clinical skills and sophisticated radiological imaging. The aim of reconstruction of the facial fractures is to rehabilitate the patient both functionally and aesthetically. In this article we employed B-spline curves to construct the occipital bone fracture using Digital Imaging and Communications in Medicine (DICOM) format data. The construction of occipital bone fracture starts with the boundary extraction followed by corner detection, construction of fractured part inner outer curve for each DICOM data using B-spline curves and finally the construction of fractured part in DICOM format. Method used in this article is based on DICOM data only and does not require any technique such as mirror imaging, technical help, reference skull, or to take average thickness of skull bone. Using the proposed method, the constructed fractured implant is custom made for every individual patient. At the end of this article we present a real case, in which we have constructed the occipital bone fracture using B-spline. The proposed method has been validated using post-operation DICOM data. For practical application, Graphical User Interface (GUI) has been developed.

Keywords CT scan DICOM data \cdot Boundary extraction \cdot B-spline curves \cdot Occipital bone defect reconstruction \cdot Graphical user interface (GUI)

Communicated by Cristina Turner.

Published online: 22 July 2017

Abdul Majeed abdulmajeed@ue.edu.pk

Division of Science and Technology, University of Education, Lahore, Pakistan

DRB-HICOM University of Automotive Malaysia, 26607 Pekan, Pahang, Malaysia

Institute of Engineering Mathematics, Universiti Malaysia Perlis, Pauh Putra Campus, 02600 Pauh, Perlis, Malaysia

Craniofacial Medical Imaging Research Group, School of Dental Sciences, Universiti Sains Malaysia, 16150 Kota Bharu, Kelantan, Malaysia

National University of Science and Technology, Islamabad, Pakistan

Mathematics Subject Classification 65D17 · 65D18 · 68U07

1 Introduction

Cranio-maxillo-facial region is a complex anatomical location of the human body where reside various vital viscera. A diverse range of etiological entities can disrupt normal anatomical profile of the craniofacial region such as road traffic accidents, sports injury, tumors and congenital anomalies. Figure 1 broadly explains the various bones that join like a jig saw puzzle to construct the complex craniofacial region. It is not a surprise that the disruption of the craniofacial region secondary to trauma does not follow a pattern. Various different radiological modalities are used in practice to diagnose facial fractures such as X-rays, CT scan and MRI.

Although CAD/CAM technology has been employed to reconstruct the fractured segments of the craniofacial region (Lee et al. 2002; Mller et al. 2003), it is expensive and requires skilled technicians. Several other methods are available to design implants without CAD processing such as mirroring (Sauret et al. 2002) which works for unilateral fracture only using reference model (Shui 2010) which is not a custom made for every individual patient. Carr et al. (1997) have constructed the cranial defect using radial basis functions (RBF). Carr et al. (2001) reconstruct the 3D objects using radial basis functions. Chowdhury et al. (2009) used iterative closest point (ICP) algorithm for the construction of virtual craniofacial reconstruction. In this article, authors had constructed the mandible bone fracture taking non-fractured bone contour as a reference contour. Majeed et al. (2016) constructed the parietal bone fracture part using GC^1 rational Ball curves. For more related work, see Greef and Willems (2005), Claes et al. (2007), Tu et al. (2007), andermeulen et al. (2006) and Bhatt and Warkhedkar (2008), and references therein.

This article proposes the occipital bone fracture reconstruction using B-spline curves. Before reconstructing the fracture part we check the applicability of proposed method, by constructing the boundary curve of full skull. Mathematical morphology is used to obtain the boundary of skull. After this we reconstruct the inner and outer curves of traumatised part of all CT scan slices. Then the fractured parts are converted to DICOM format. The suggested method is time efficient, custom made for every individual patent and user friendly since there is no need to construct the reference model, to take the average thickness of skull bone and to take mirror image.

The proposed method has been validated by reconstructing self-implanted fractured part which gives the same result as the original part. We present a case report of occipital bone fracture to show the applicability and validity of proposed method. The DICOM data used in this paper are obtained from Hospital Universiti Sains Malaysia (HUSM). We employ MATLAB for both the programming and to develop Graphical User Interface (GUI) for occipital bone fracture reconstruction using proposed method. Surgeons can use GUI for fracture reconstruction without having in-depth knowledge of its mathematical aspect. The input for the GUI is knot points which can be obtained by clicking on image. The reconstructed part can be changed or adjusted by dragging the knot points.

1.1 Objectives and significance of the study

The objectives of this study are

• To provide an alternative method for the construction of occipital bone fractures.



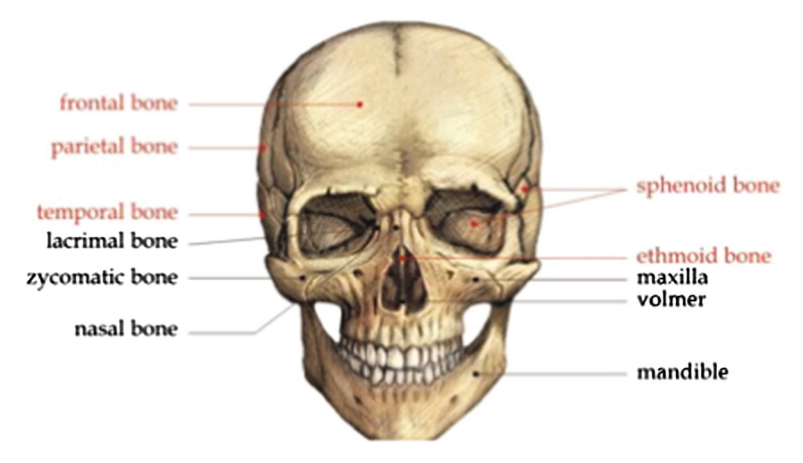


Fig. 1 Craniofacial bones

- To apply B-spline curves for the construction of fractured part boundary curves and construct the fractured part in DICOM format.
- To develop a graphical user interface for the construction of fractured part curves for those without or with limited knowledge in mathematics.
- To provide the method for custom-made implant.

This study is significant because

- This study will provide the methods to construct the required thickness of bone.
- This study will provide the custom-made implant for every unique patient.
- This study will provide the best solution or treatment option for the benefit of the patient.

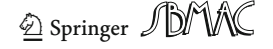
2 Theoretical foundation

With the advent of modern technologies in various fields and technology oriented business environment the use of computers has become a dire need and to implement the algorithms and 3D designing of various products computer-aided geometric design (CAGD) has played a vital role. CAGD or another term called geometric modeling refers to the research stream for the development and representation of different forms of curves, surfaces in free form.

The concept of CAGD emerged in 1970s and expanded in diverse fields ranging from automotive industry to aerospace rapid prototyping machines. Barnhill and Riesenfeld are considered to be the pioneers of this field when they organized a conference to discuss different aspects of CAGD at University of Utah, USA in 1974.

After this conference, this field evolved in a systematic manner with enhanced features and insights into different technological aspects. In this context, first formal book on this topic appeared in the literature with the title Computational Geometry for Design and Manufacturing authored by Faux and Pratt (1979) and was based on the previous fundamental work of Coons (1964) and De Casteljau (1959).

The CAGD was first developed for hard core technology such as automobiles and aeronautics to implement the complicated designs of various components and assemblies. However, since the last decade, CAGD has become a mature technology and is being used in various technologies especially having complicated designs including bio-modeling. The B-spline basis functions have been used in this work for occipital bone fracture reconstruction.



2.1 B-spline basis functions and curves

There are different ways to define and prove the important properties of B-spline basis. For example, Curry et al. (1947) defined B-spline basis by divided difference of truncated power functions. Ramshaw (1987) defined it by blossoming. Cox (1972) and De Boor (1972, 1978) defined B-spline basis functions by recurrence formula. For the current study, recurrence formula is used to define the B-spline basis. B-spline curves and surface methods were suggested for the first time in 1940s. But in 1970s, several researches, especially R. Riesenfeld, developed B-spline curves and surfaces methods.

The B-spline curves surmount the disadvantages of Bezier curves like:

- Bezier curve degree is dependent on the number of control points while the degree of B-spline is independent of control points.
- Bezier curve has a global control while B-spline curve has a local control.
- It is easy to achieve the C^1 continuity between two Bezier curve segments but tough to get C^2 continuity, while in B-spline, if individual curve segment has degree n then it attains the C^{n-1} continuity between two B-spline segments.

In this paper, cubic B-spline curves will be used to reconstruct the occipital bone fractures. To fit the cubic B-spline curve, control points and cubic B-spline basis are required.

The B-spline basis functions of degree d, denoted $N_{i,d}(t)$, defined on the knot vector t_0, \ldots, t_m are defined recursively as follows:

$$N_{i,0}(t) = \begin{cases} 1, & \text{if } t \in [t_i, t_{i+1}), \\ 0, & \text{otherwise.} \end{cases}$$
 (1)

$$N_{i,d}(t) = \frac{t - t_i}{t_{i+d} - t_i} N_{i,d-1}(t) + \frac{t_{i+d+1} - t}{t_{i+d+1} - t_{i+1}} N_{i+1,d-1}(t)$$
 (2)

for $i = 0, \ldots, n$ and $d \ge 1$.

The uniform cubic B-spline basis function with d = 0, ..., 3 are shown in Fig. 2.

Theorem 1 The B-spline basis functions $N_{i,d}(t)$ obey the following properties:

Positivity The B-spline basis are always positive $N_{i,d}(t) > 0$ for $t \in (t_i, t_{i+d+1})$.

Local support *B-spline has a local support* $N_{i,d}(t) = 0$ *for* $t \notin (t_i, t_{i+d+1})$ *as shown in* Fig. 2. In particular, Fig. 2d, $N_{2,3}(t)$ is non-zero for $t \in (2,6)$ otherwise it is zero.

Piecewise polynomial The B-spline basis $N_{i,d}(t)$ are piecewise polynomial functions of degree d as shown in Fig. 2.

Partition of unity The B-spline basis functions obey the partition of unity property as the sum of all basis is 1. $\sum_{i=r-d}^{r} N_{j,d}(t) = 1$. for $t \in [t_r, t_{r+1})$.

Continuity If interior knot t_i has multiplicity p_i , then $N_{i,d}(t)$ is C^{d-p_i} at $t = t_i$. $N_{i,d}(t)$ is C^{∞} elsewhere (Fig. 3).

Theorem 2 A B-spline curves $P(t) = \sum_{i=0}^{n} b_i N_{i,d}(t)$ of degree d defined on the knot vector t_0, \ldots, t_m satisfy the following properties:

Local control Each segment is determined by d+1 control points. If $t \in [t_r, t_{r+1})(d \le r \le m-d-1)$, then $P(t) = \sum_{i=r-d}^r b_i N_{i,d}(t)$. Thus, to evaluate P(t) it is sufficient to evaluate $N_{r-d,d}(t), \ldots, N_{r,d}(t)$.

Effect of control points By changing the P_0 control point only first segment will change, remaining segments of curve will remain the same as shown in Fig. 4. By changing the position of P_2 control points, two curve segments $P_3(t)$ and $P_4(t)$ will change as shown in Fig. 5.



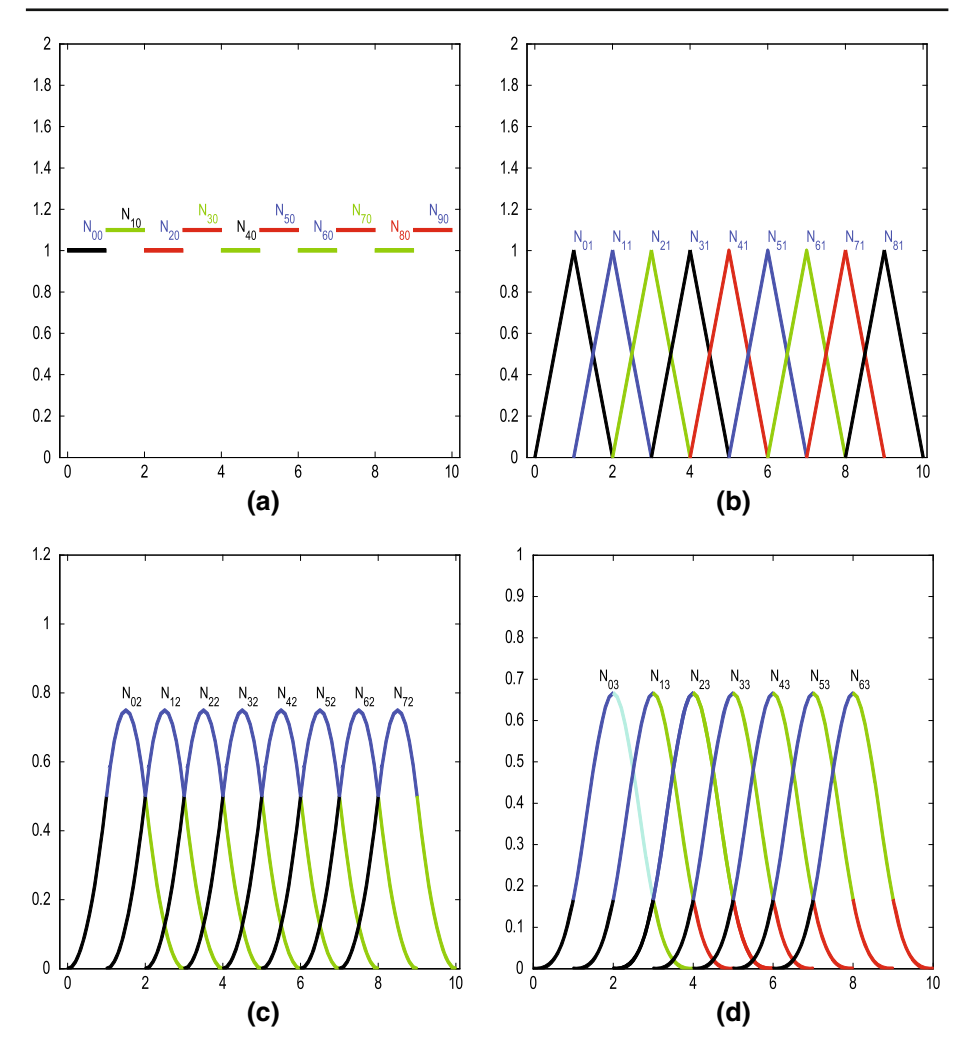


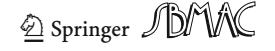
Fig. 2 Uniform cubic B-spline basis functions $\mathbf{a} d = 0$, $\mathbf{b} d = 1$, $\mathbf{c} d = 2$, $\mathbf{d} d = 3$

Convex hull property *B-spline curves obey the convex hull property. It means that curves formed by B-spline basis always lie within the convex hull of their control points as shown in Fig.* 3.

Continuity If p_i is the multiplicity of the break point $t = u_i$, then P(t) is C^{d-p_i} at $t = u_i$ and C^{∞} elsewhere. In this article we use cubic B-spline so at each knot there is a C^2 continuity as shown in Fig. 3. The continuity will reduce to C^1 at a particular point where we repeat the knot as shown in Fig. 6. The continuity will become C^0 if we repeat two knots at a point as shown in Fig. 7. Similarly, if we repeat three knots at a point it will give us two disjoint B-spline curve segments as shown in Fig. 8.

Invariance under affine transformation *Let* T *be an affine transformation. Then* $T(\sum_{i=0}^{n} b_i N_{i,d}(t)) = \sum_{i=0}^{n} T(b_i) N_{i,d}(t)$.

B-spline is said to be uniform if knots are equally spaced. In this article we use uniform B-spline of degree 3 with knots $t_0 = 0$, $t_1 = 1$, $t_2 = 2$, ... $t_m = m$. The basis functions for uniform cubic B-spline are



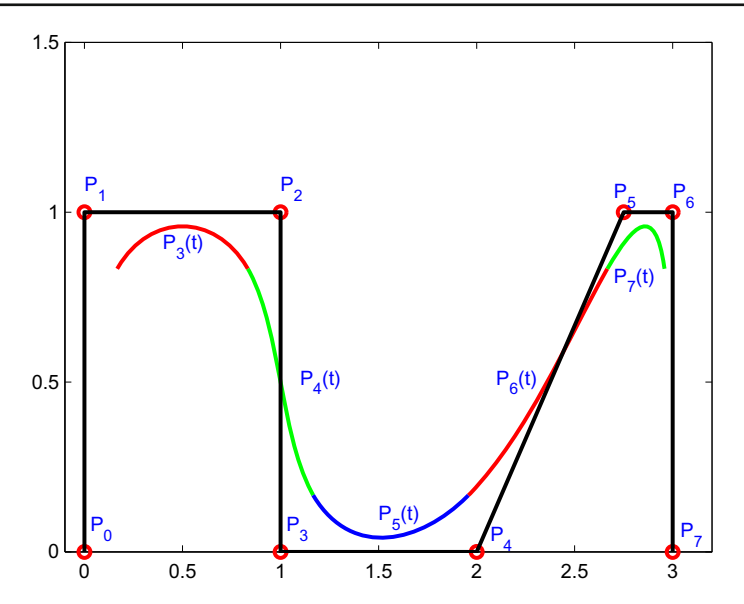


Fig. 3 B-spline curve

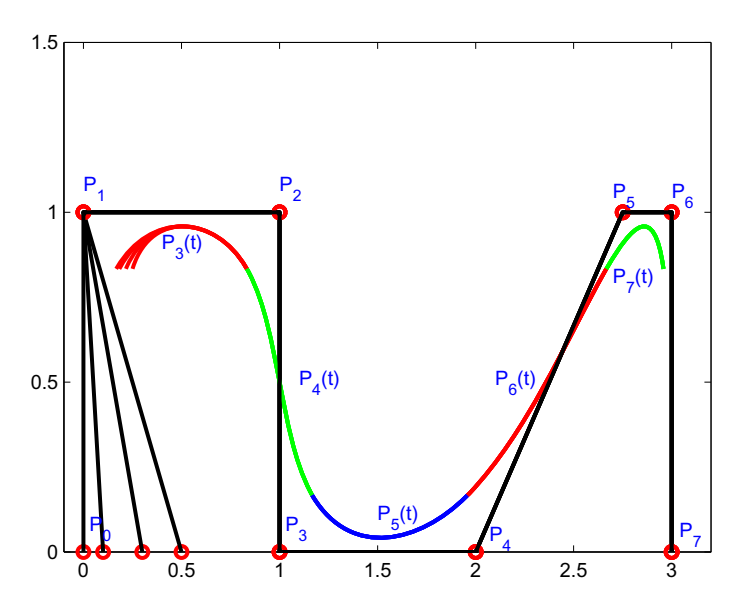


Fig. 4 B-spline curve with different P_0 control point

$$N_{i,0}(t) = \begin{cases} 1, & \text{if } t \in [t_i, t_{i+1}), \\ 0, & \text{otherwise.} \end{cases}$$

The *i*th basis functions for degree 3 are

$$N_{i,3}(t) = \frac{(t-i)^3}{6} N_{i,0}(t) + \left[\frac{(t-i)^2(i+2-t)}{6} + \frac{(t-i)(i+3-t)(t-i-1)}{6} + \cdots + \frac{(t-i-1)^2(i+4-t)}{6} \right] N_{i+1,0}(t) + \left[\frac{(t-i)(i+3-t)}{6} + \cdots + \frac{(t-i)(i+3-t)}{6} + \cdots + \frac{(t-i)(i+3-t)(t-i-1)}{6} +$$



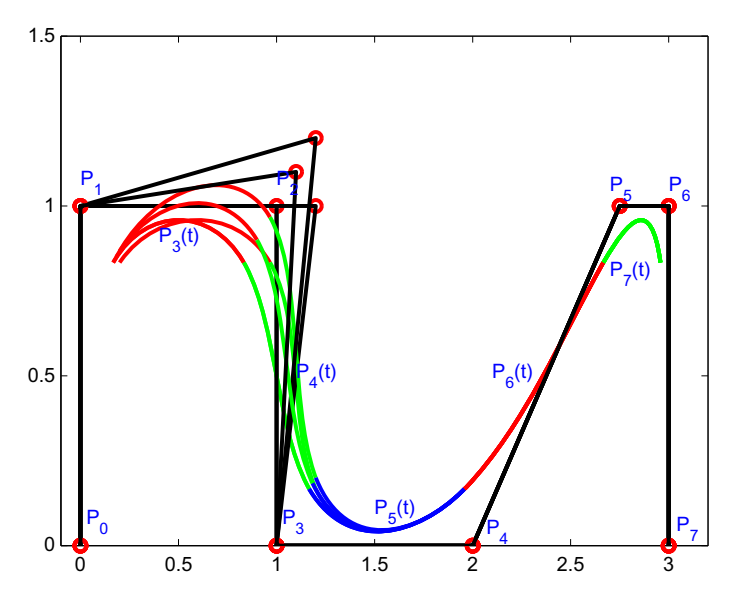


Fig. 5 B-spline curve with different P_2 control point

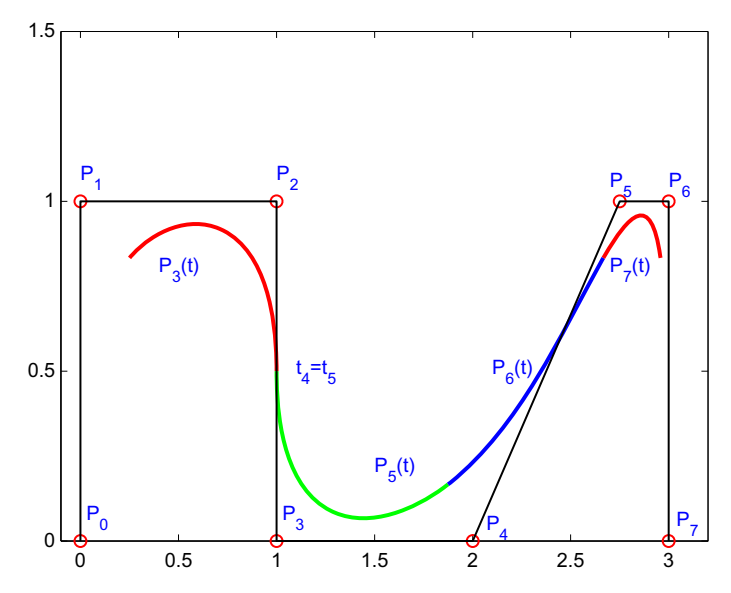


Fig. 6 B-spline curve with $t_4 = t_5$

$$+\frac{(i+3-t)(i+4-t)(t-i-1)}{6} + \cdots + \frac{(t-i-2)(i+4-t)^2}{6}$$

$$\times N_{i+2,0}(t) + \frac{(i+4-t)^3}{6} N_{i+3,0}(t).$$



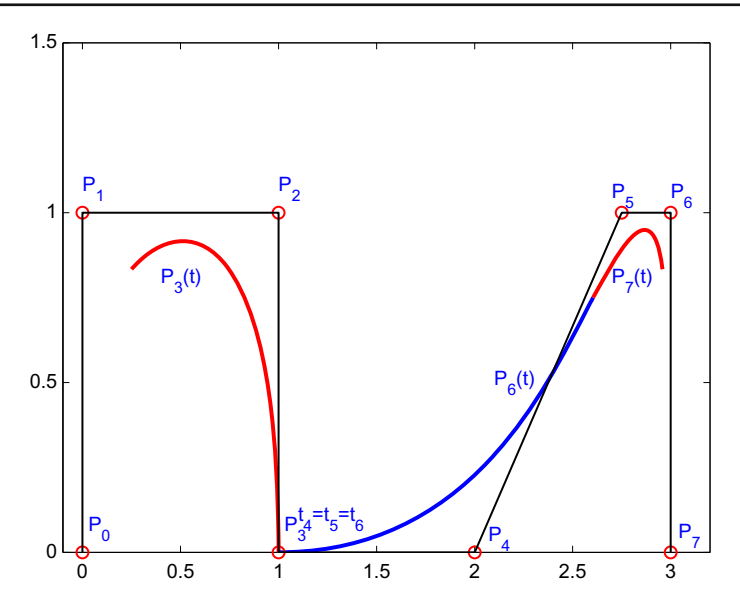


Fig. 7 B-spline curve with $t_4 = t_5 = t_6$

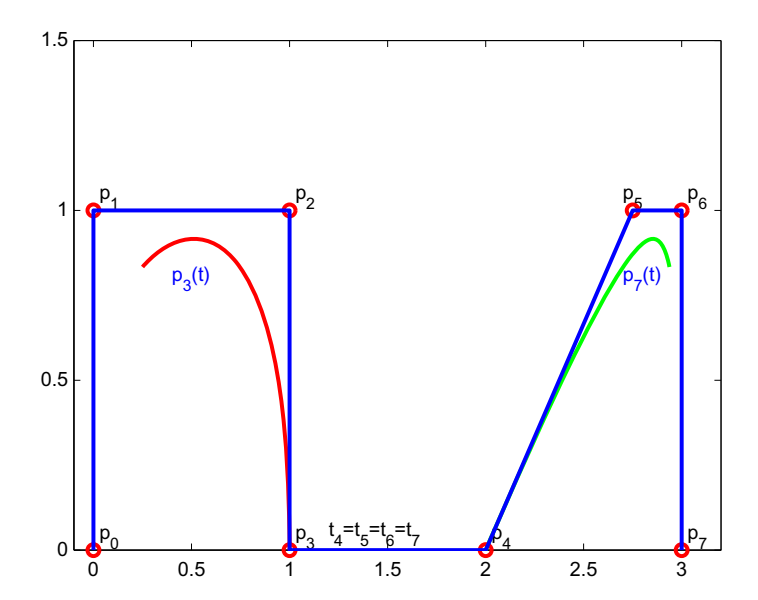


Fig. 8 B-spline curve with $t_4 = t_5 = t_6 = t_7$

Thus, the ith segment $Q_i(t)$ of B-spline curve defined on [i+3, i+4) is

$$Q_i(t) = \sum_{j=i}^{i+3} P_j N_{j,3}(t) \frac{(i+4-t)^3}{6} P_0 + \left[\frac{(t-i-1)(i+4-t)^2}{6} + \frac{(i+4-t)(i+5-t)(t-i-2)}{6} \right]$$



$$+ \cdots \frac{(t-i-3)(i+5-t)^2}{6} \right] P_1 + \left[\frac{(t-i-2)^2(i+4-t)}{6} + \frac{(t-i-3)(i+5-t)(t-i-2)}{6} + \cdots + \frac{(t-i-3)^3(i+6-t)}{6} \right] P_2 + \frac{(t-i-3)^3}{6} P_3.$$

By re-parameterization $t \to t + i + 3$ define the segment on the interval [0, 1]

$$Q_i(t) = \frac{(1-t)^3}{6} P_0 + \frac{(3t^3 - 6t^2 + 4)}{6} P_1 + \frac{(-3t^3 + 3t^2 + 3t + 1)}{6} P_2 + \frac{t^3}{6} P_3.$$
 (3)

In matrix form we can write it as

$$Q_{i}(t) = \frac{1}{6}(t^{3} t^{2} t 1) \begin{bmatrix} -1 & 3 & -3 & 1 \\ 3 & -6 & 3 & 0 \\ -3 & 0 & 3 & 0 \\ 1 & 4 & 1 & 0 \end{bmatrix} \begin{bmatrix} P_{i} \\ P_{i+1} \\ P_{i+2} \\ P_{i+3} \end{bmatrix}.$$
(4)

Equation 3 is the generalized uniform B-spline curve, which we will use in this paper. For close curve, Eq. 3 becomes

$$Q_{i}(t) = \frac{1}{6}(t^{3} t^{2} t 1) \begin{bmatrix} -1 & 3 & -3 & 1 \\ 3 & -6 & 3 & 0 \\ -3 & 0 & 3 & 0 \\ 1 & 4 & 1 & 0 \end{bmatrix} \begin{bmatrix} P_{(i-1)mod(n+1)} \\ P_{(i+1)mod(n+1)} \\ P_{(i+2)mod(n+1)} \\ P_{(i+3)mod(n+1)} \end{bmatrix}.$$
 (5)

To find the control points, the boundary of CT scan image is required which is obtained using mathematical morphology. The corner points convert the boundary in segments. The start and end points of each segment were used as a knot point in B-spline curves. In other words, it can be established that knot points are the position of the transitions between curve segments. The parameter t defined each curve segment over the interval [0, 1]. Hence, the one curve segment will change to next curve segment at t = 0 and t = 1. From Eq. (3), $Q_i(0)$ can be written in the form of control points. For a closed cubic B-spline curve, we can write it as:

$$\begin{bmatrix} Q_{i}(0) \\ Q_{i+1}(0) \\ Q_{i+2}(0) \\ \vdots \\ Q_{n-1}(0) \\ Q_{n}(0) \\ Q_{n+1}(0) \end{bmatrix} = \frac{1}{6} \begin{bmatrix} 1 & 4 & 1 & \cdots & 0 & 0 & 0 \\ 0 & 1 & 4 & \cdots & 1 & 0 & 0 \\ 0 & 0 & 1 & \cdots & 4 & 1 & 0 \\ \vdots & \vdots & & \vdots & \vdots & & \vdots & \vdots \\ 0 & 0 & 0 & \cdots & 1 & 4 & 1 \\ 1 & 0 & 0 & \cdots & 0 & 1 & 4 \\ 4 & 1 & 0 & \cdots & 0 & 0 & 1 \end{bmatrix} \begin{bmatrix} P_{i} \\ P_{i+1} \\ P_{i+2} \\ \vdots \\ P_{n-1} \\ P_{n} \\ P_{n+1} \end{bmatrix}.$$
(6)

The control points are as

$$\begin{bmatrix}
P_{i} \\
P_{i+1} \\
P_{i+2} \\
\vdots \\
P_{n-1} \\
P_{n} \\
P_{n+1}
\end{bmatrix} = 6
\begin{bmatrix}
1 & 4 & 1 & \cdots & 0 & 0 & 0 \\
0 & 1 & 4 & \cdots & 1 & 0 & 0 \\
0 & 0 & 1 & \cdots & 4 & 1 & 0 \\
\vdots & \vdots & & \vdots & \vdots & \vdots & \vdots \\
0 & 0 & 0 & \cdots & 1 & 4 & 1 \\
1 & 0 & 0 & \cdots & 0 & 1 & 4 \\
4 & 1 & 0 & \cdots & 0 & 0 & 1
\end{bmatrix}
\begin{bmatrix}
Q_{i}(0) \\
Q_{i+1}(0) \\
Q_{i+2}(0) \\
\vdots \\
Q_{n-1}(0) \\
Q_{n}(0) \\
Q_{n+1}(0)
\end{bmatrix}$$
(7)



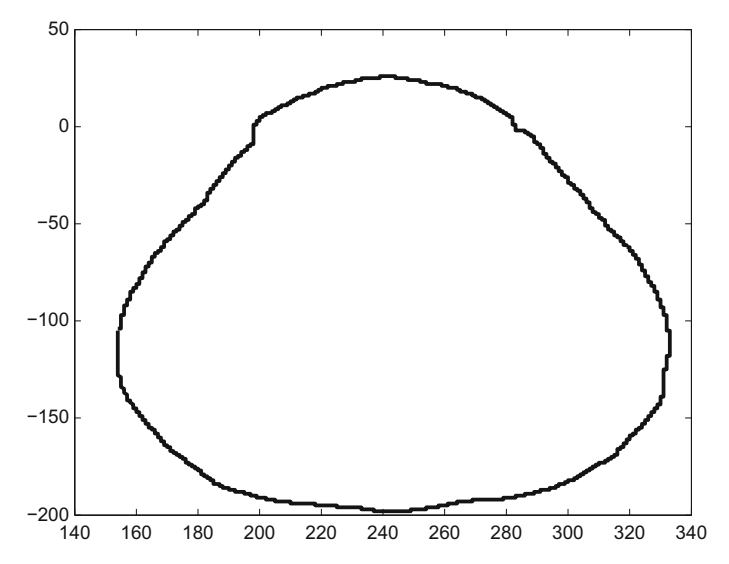


Fig. 9 Boundary of CT Scan image

For open curve, let $Q_0 = P_0$ and $Q_n = P_n$. The remaining control points can be defined as

$$\begin{bmatrix} P_1 \\ P_2 \\ P_3 \\ \vdots \\ P_{n-3} \\ P_{n-2} \\ P_{n-1} \end{bmatrix} = \begin{bmatrix} 4 & 1 & 0 & \cdots & 0 & 0 & 0 \\ 1 & 4 & 1 & \cdots & 0 & 0 & 0 \\ 0 & 1 & 4 & \cdots & 1 & 0 & 0 \\ \vdots & \vdots & & \vdots & \vdots & & \vdots & \vdots \\ 0 & 0 & 0 & \cdots & 1 & 4 & 1 \\ 0 & 0 & 0 & \cdots & 1 & 4 & 1 \\ 0 & 0 & 0 & \cdots & 0 & 1 & 4 \end{bmatrix}^{-1} \begin{bmatrix} 6Q_1 - Q_0 \\ 6Q_2 \\ 6Q_3 \\ \vdots \\ 6Q_{n-3} \\ 6Q_{n-2} \\ 6Q_{n-1} - Q_n \end{bmatrix}, \tag{8}$$

where P_i , $0 \le i \le n$ are required control points and Q_i , $0 \le i \le n$ are given boundary data points.

There are two ways to adjust the control points: first by taking maximum number of control points, starting curve fitting and then removing the redundant control points. Second, start fitting by taking small number of control points and increase the control points as required. In this article we start fitting with the small number of control points. As an example we use the boundary of 2D CT scan skull image as shown in Fig. 9. We start B-spline curve fitting using ten control points which are the corner points as shown in Fig. 10. In this figure, red curve is the B-spline curve and black is the original. To get the best fit we increase the control points to 17 as shown in Fig. 11 and finally to 20 as shown in Fig. 12.

The construction of the frontal bone fractured part using C^1 rational ball curve has been presented by Majeed et al. (2015) and have taken tangents at the end points. The intermediate control points are defined by tangent vectors. The method works well for small fractures area. In case of large fractures, it gives tight curve; however, by breaking the large fractured parts into segments, it produces good results but at high computational cost. At the same time, it is not convenient to evaluate intermediate control points and, therefore, it becomes difficult to handle free shape parameters in these segmented parts especially for non-mathematicians.



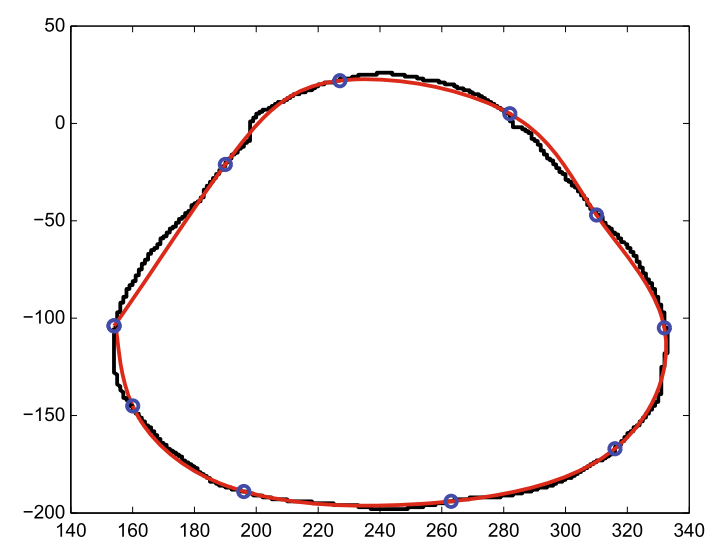


Fig. 10 B-spline curve fitting with 10 knots

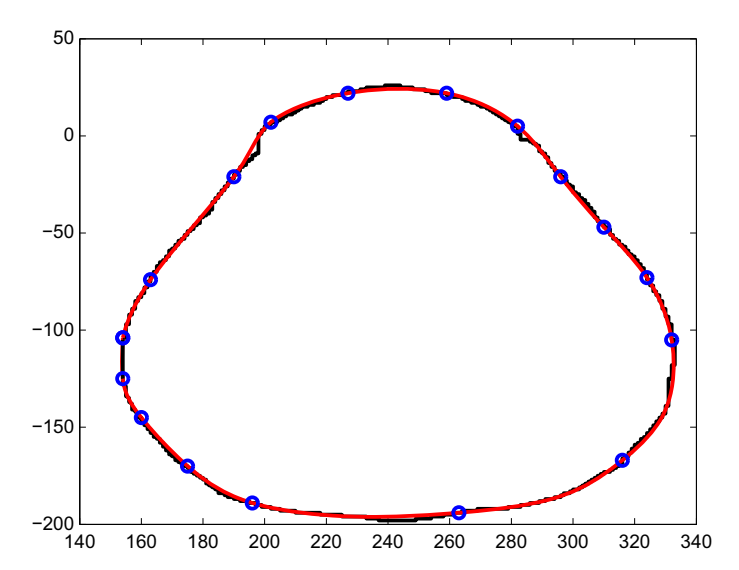


Fig. 11 B-spline curve fitting with 17 knots

In this paper, the authors address all these issues and introduce the proposed method that is not only efficient but also works equally good for small and large fractured parts. Moreover, the method uses only knot points as input that is independent of free shape parameters. In this method, the control for dividing the fractured part into segments rests with user until the desired results are achieved by him/her. The GUI in current work is more efficient and construction is just based on clicking the given image. The constructed fractured part can be changed by dragging or increasing the knot points.



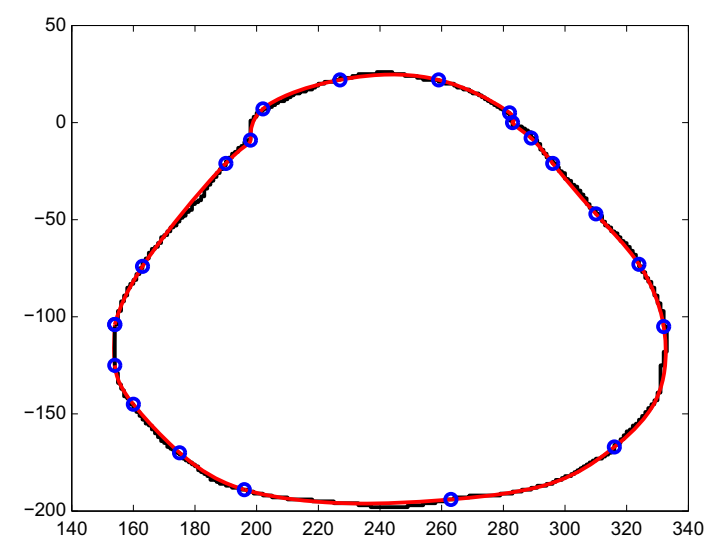


Fig. 12 B-spline curve fitting with 20 knots

2.2 Boundary extraction and corner detection

To construct the occipital bone fracture, initially we will extract the boundary of each CT scan image. Mathematical morphology defined by Majeed and Piah (2014) is used to obtain the boundary of each image which is defined as $\beta(A) = A - (A\Theta B)$.

To divide the boundary in smaller segments we use the corner points. Sarfarz et al method (2006) is used to find the corner points. After constructing the traumatized part, next step is to convert the fractured part into DICOM format; for this, method defined by Majeed et al. (2015) has been used.

2.3 Graphical user interface (GUI)

GUI consists of one or more windows having controls, these are called components. GUI is utilized to perform the interactive tasks and display it graphically. GUI facilitates the users in completion of different tasks. Users are not required to learn the basic programming of each component. GUI consists of start and stop button, panel, scroll bar, push button, boxes, etc.

GUI and each of its control have an executable MATLAB code known as callbacks. The implementation of each callback is activated by a particular user action such as clicking a mouse button, pressing a screen button, typing a string or a numeric value, selecting a menu item, or passing the cursor over a component. The GUI then reacts to these events. In this article, we have constructed the GUI using B-spline curves. The input for curve construction is knot points only. The constructed curves can be changed and controlled by dragging and increasing the knot points.

3 Case study: reconstruction of occipital bone fracture

This section explains the method for the construction of occipital bone fracture using B-spline. The CT scan data of patient with brain tumor in DICOM format are shown



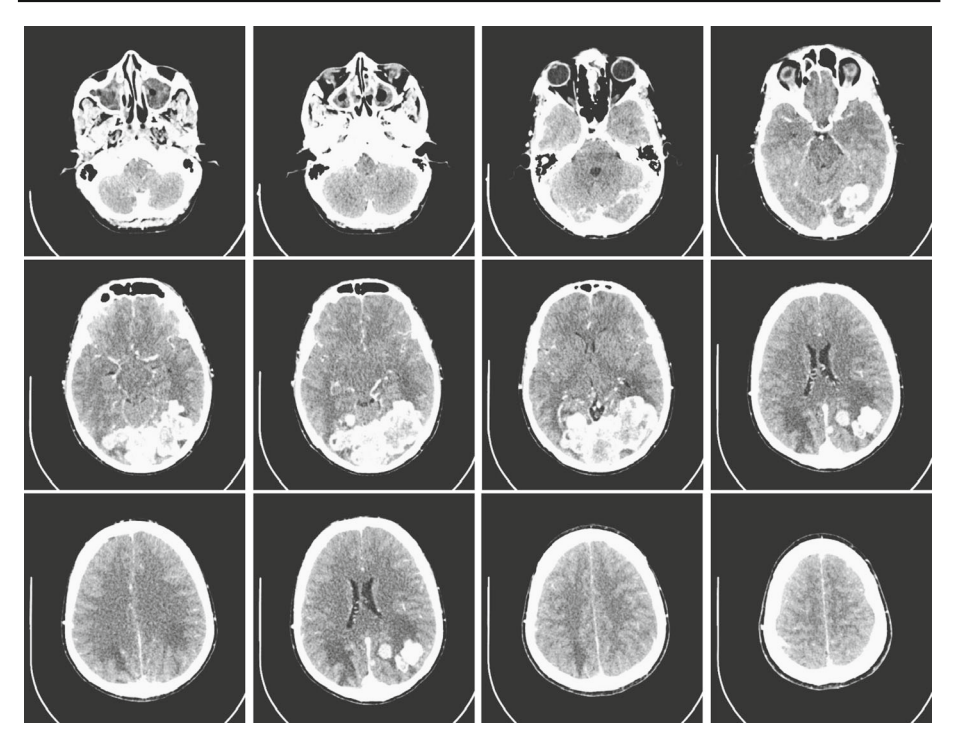


Fig. 13 CT scan images of patient with brain tumor

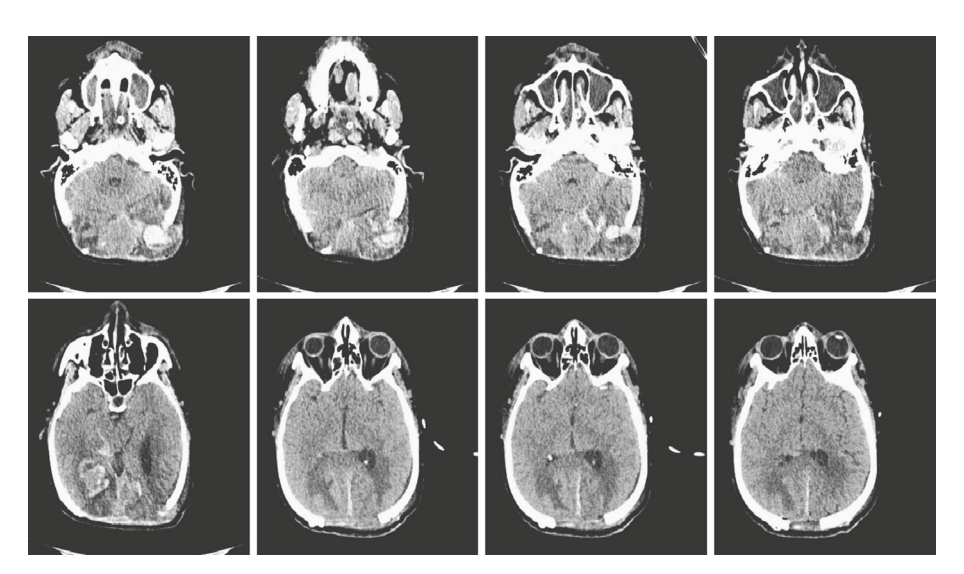


Fig. 14 CT scan images of patient after operation

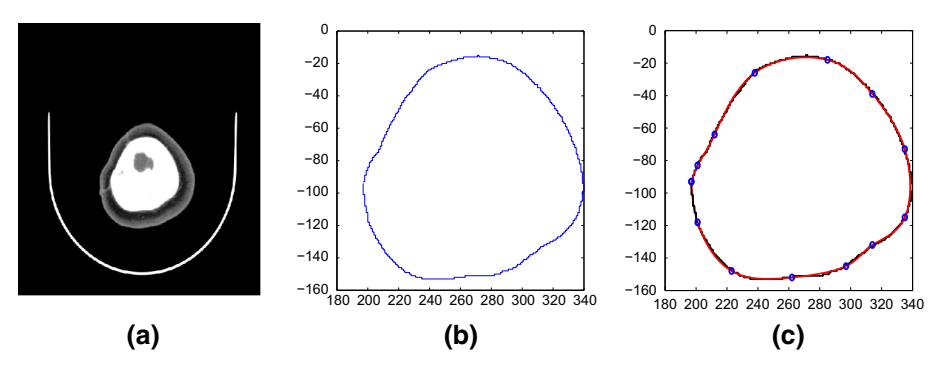


Fig. 15 Reconstructed boundary a original image, b boundary, c full skull boundary curve reconstruction using B spline curves curve

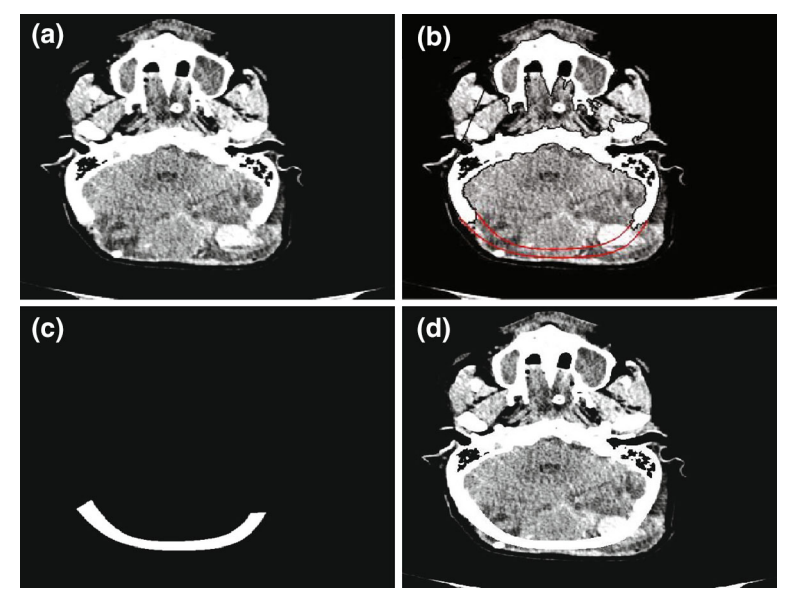


Fig. 16 Construction of fractured part using B spline

in Fig. 13. To treat brain tumor, the neurosurgeon has resected the occipital bone as shown in Fig. 14 which has been used for this study. To test the applicability of proposed method, first we reconstruct the boundary curve of complete skull (non-fractured skull contour) as shown in Fig. 15. First step to construct the complete skull is to extract the boundary of skull as shown in Fig. 15b. Corner points divide the boundary curve into segments as shown in Fig. 15c. The corner points are also considered as a knot points which helps in evaluating the control points for B-spline curves. After finding the control points, the boundary curve for each segment has been reconstructed using B-spline as shown in Fig. 15c. In this figure, red curve is reconstructed and black is original.

After reconstructing the complete skull, we used B-spline curves to construct the fractured part as shown in Fig. 16. This figure explains the detail steps for the construction of fractured part in DICOM format. In this figure (a) is the CT scan image and (b) shows the reconstructed boundary curves of fractured part using B-spline. The input for curve construction is knot



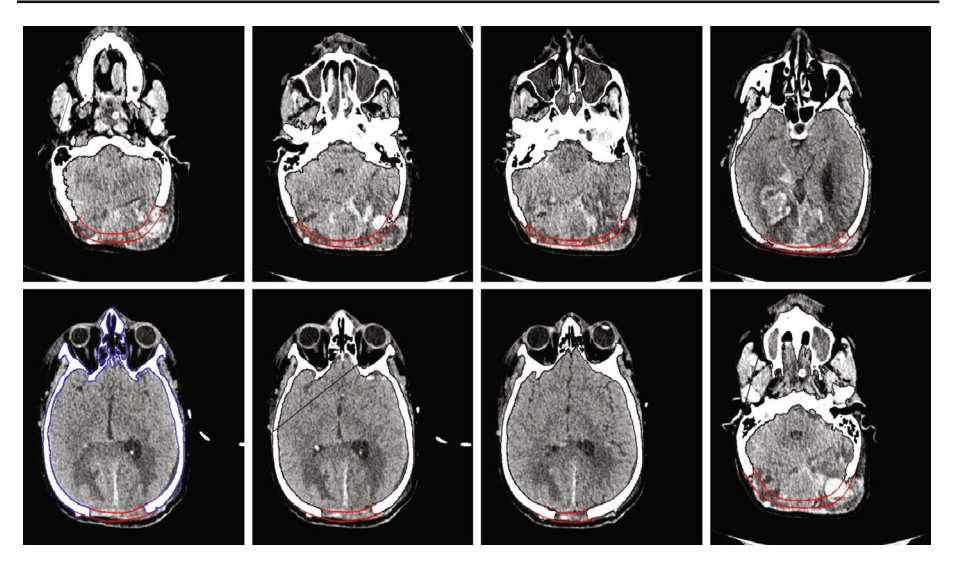


Fig. 17 Construction of fractured part curves for different CT scan images using B-spline curves

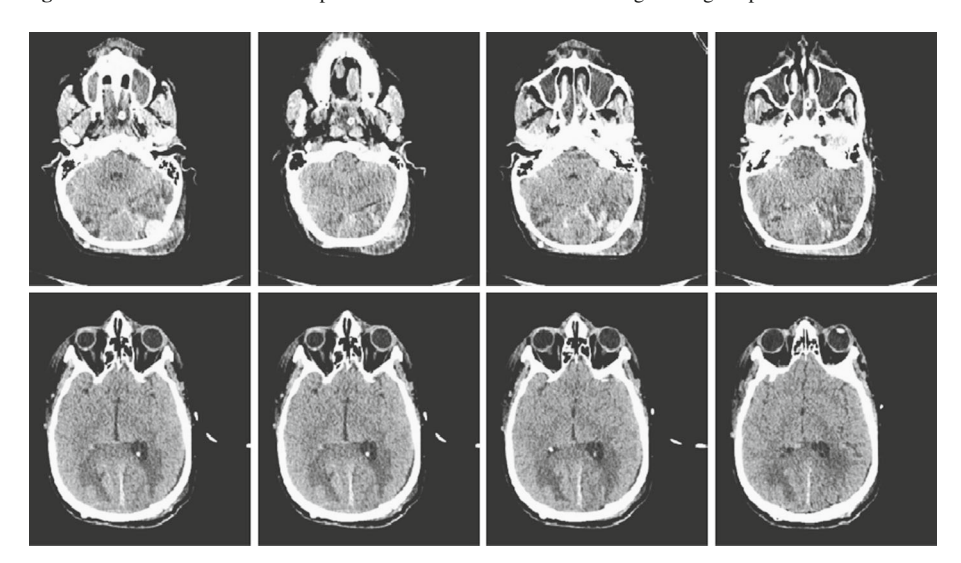
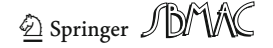


Fig. 18 Construction of fractured part in DICOM format for different CT scan images

points only. We can adjust or change the constructed curves by changing the position of knot points. Further curves can be handled by increasing the number of knot points if required. The fractured part in DICOM format is represented in (c) and (d) represents the required fractured part in DICOM format along with original image. The boundary curves of fractured part for different CT scan images are represented in Fig. 17. The construction of fractured part in DICOM format for different CT scan slices is represented by Fig. 18. To make the proposed method practically applicable for doctors and surgeons without understanding the mathematics, we have constructed the GUI using the proposed method as shown in Fig. 19. To construct fractured part curves using GUI, press insert point button and click on image for knot points where user wants the curves and click enter button on keyboard to construct



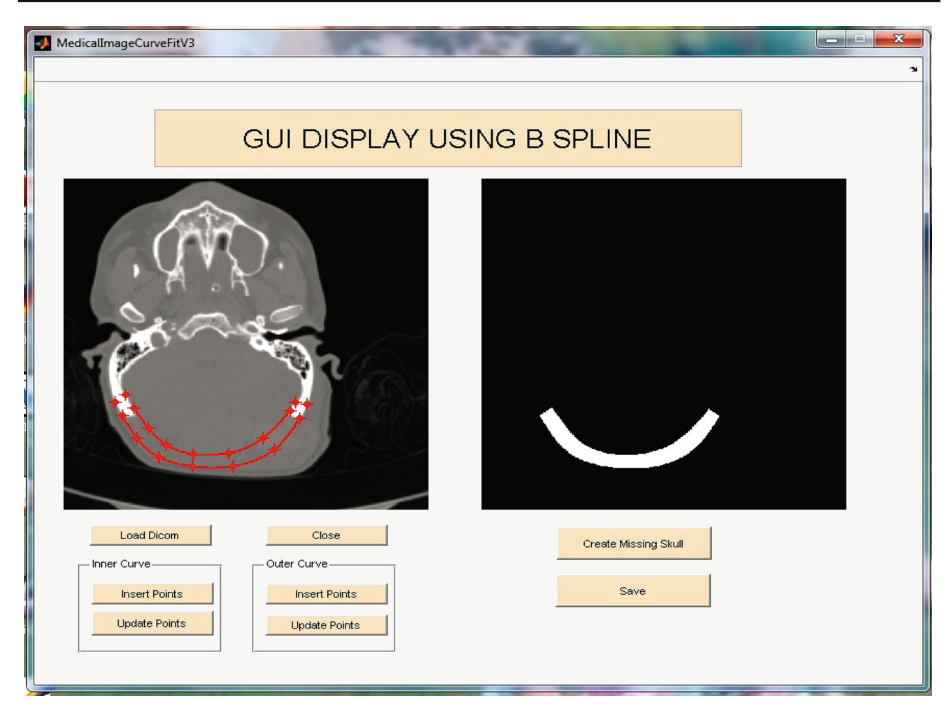


Fig. 19 GUI display of craniofacial reconstruction

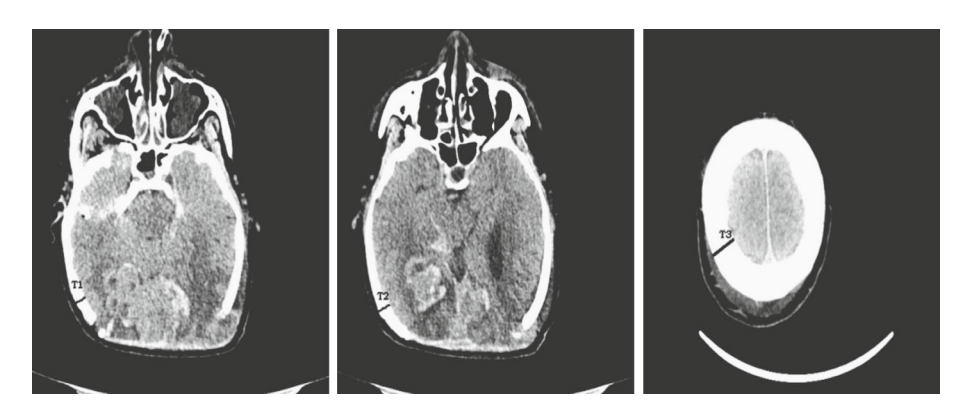


Fig. 20 Thickness of different CT scan images

curves. After getting both curves, press create missing skull button to get required fractured part in DICOM format. If the obtained fractured part is not satisfactory, the user needs to go back and click the update data point button and drag the points to required position and press enter, the curve will follow the changed points. Then press create missing skull button. Finally, press save button to save the constructed fractured part.

There is different thickness of skull bone in every slice and it also varies with its position. Figure 20 shows three images of the same patient and with different positions. The thickness varies in each image as shown in Fig. 21. In the proposed method we do not need to require to take average thickness, rather it can be calculated as shown in Fig. 21.



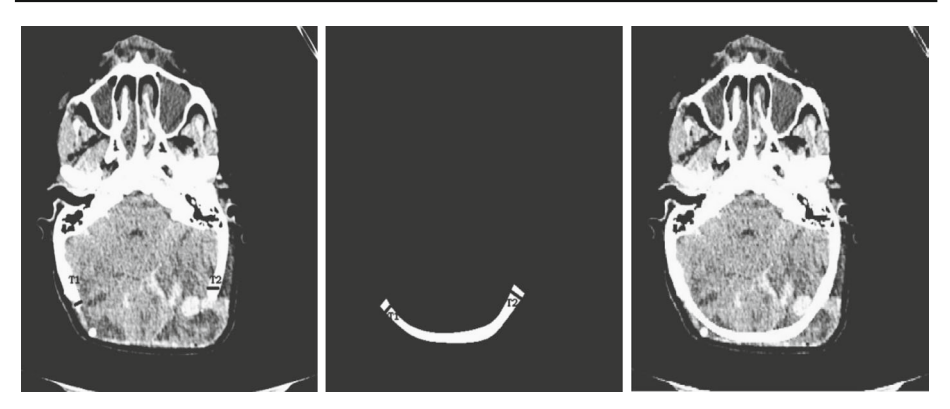


Fig. 21 Thickness of a CT scan image from different positions

3.1 Validity of proposed method

To validate the proposed method we used the post-operative CT scan images in which the neurosurgeon performed cranioplasty to insert patient bone flap to cover the defect as shown in Fig. 22. For validation of the proposed method, we follow the proposed algorithm to reconstruct the defect part. For this, fist we reconstruct the cranial implant boundary curves of one CT scan image as shown in Fig. 23b. The reconstructed cranial implant in DICOM format for this image is shown in Fig. 23c. Part (d) is combine image of (a) and (c). The reconstructed cranial implant overlaps the re-implanted skull, which shows the validity of proposed method. Furthermore, we have constructed the boundary curves for different CT scan images as shown in Fig. 24. Figure 25 represents the cranial implant in DICOM format for different CT scan images.

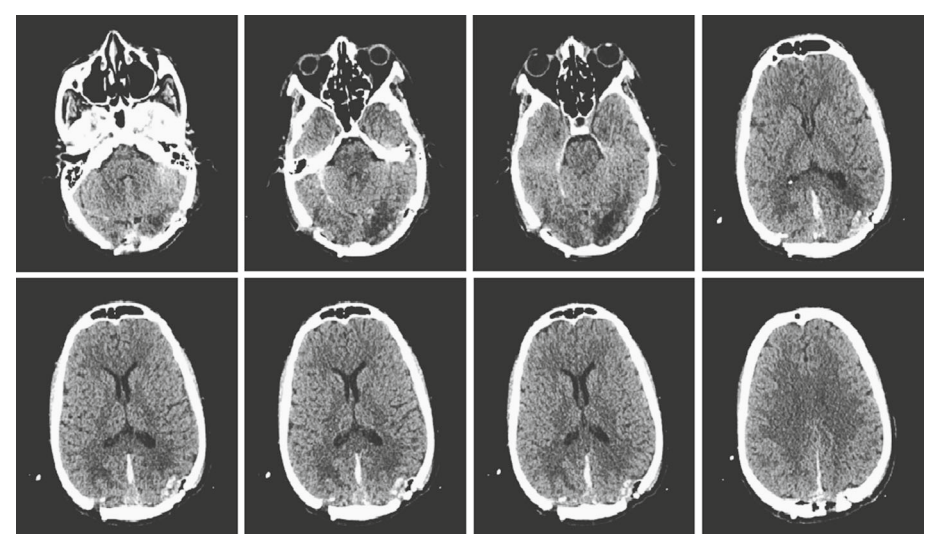


Fig. 22 Post-operative CT scan images of patient

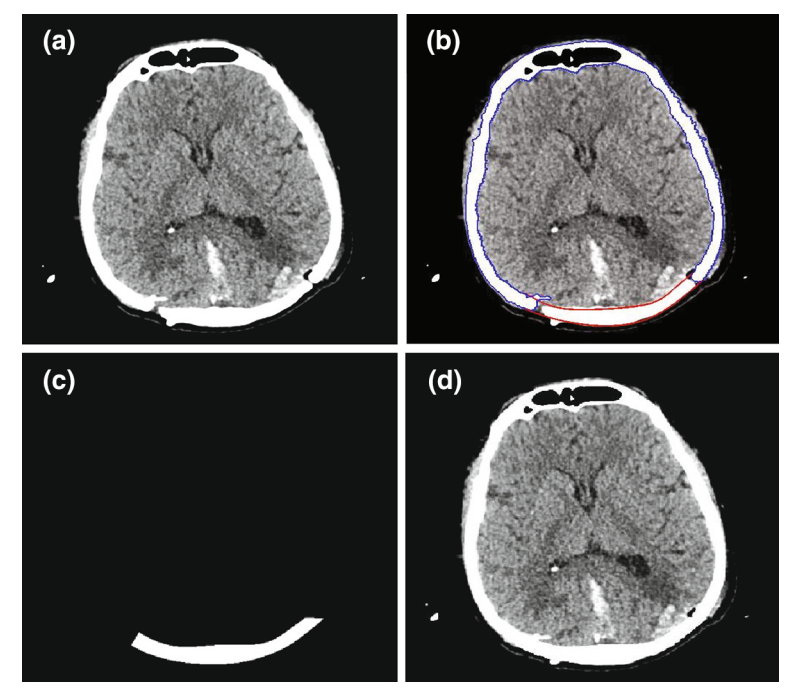


Fig. 23 Reconstruction of cranial implant

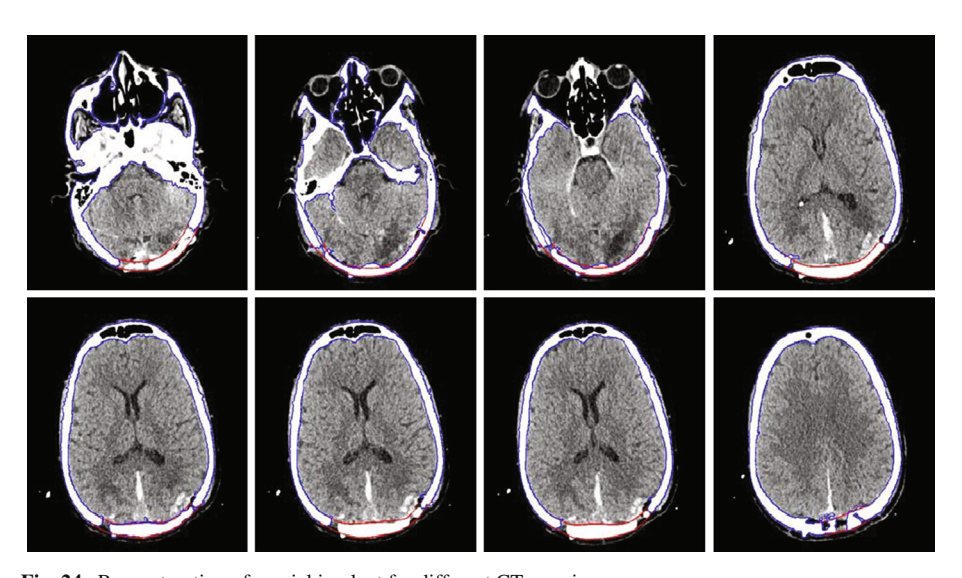


Fig. 24 Reconstruction of cranial implant for different CT scan images



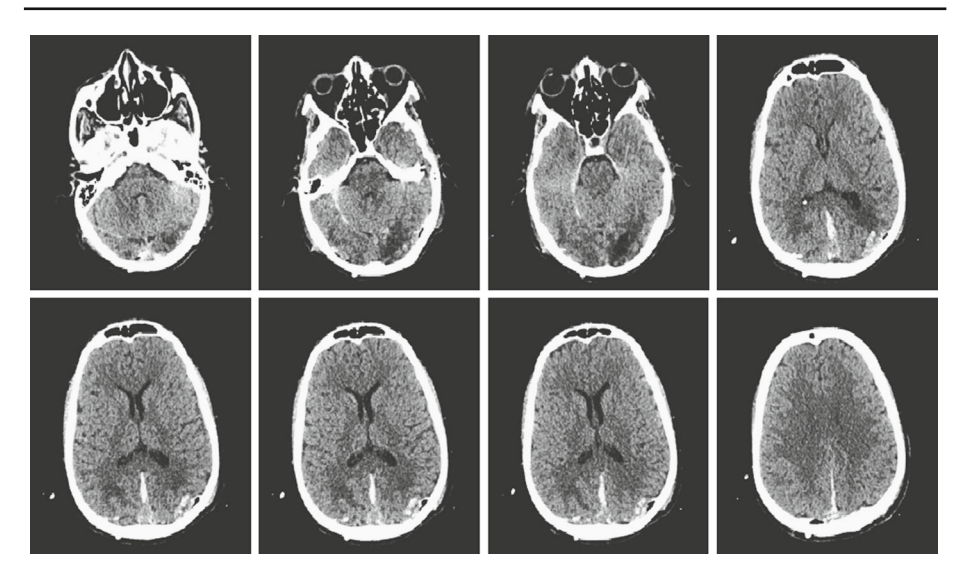


Fig. 25 Reconstruction of cranial implant in DICOM format

4 Conclusion

In this paper, B-spline curves have been used to reconstruct the occipital bone defect of real patient. The proposed method is user friendly for neurosurgeons and physicians as it does not require mirror imaging, to reconstruct reference skull model, to take the average thickness of skull bone and the construction is just based on the 2D CT scan DICOM data. The method has been validated by real-time DICOM data. Using the proposed method, the constructed cranial implant is custom made for every individual patient and we can attain the required thickness of fractured part. To facilitate physicians, GUI has been constructed.

Acknowledgements The authors would like to extend their gratitude to the Ministry of Education of Malaysia and Universiti Sains Malaysia for supporting this work under its USM Research University Grant, Account No. 1001/PPSG/852004. The authors would also like to acknowledge Dr. Hassan Iqbal's (Resident Oral and Maxillofacial Surgery in Pakistan) input in reading this article and supporting us in elaborating it.

References

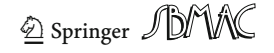
Bhatt AD, Warkhedkar RM (2008) Reverse engineering of human body: a B-spline based heterogeneous modeling approach. Comput Aided Des Appl

Carr JC, Beatson RK, Cherrie JB, Mitchell TJ, Fright WR, McCallum BC, Evans TR (2001) Reconstruction and representation of 3D objects with radial basis functions. In: Proceedings of the 28th annual conference on Computer graphics and interactive techniques 67-76. ACM

Carr JC, Fright WR, Beatson RK (1997) Surface interpolation with radial basis functions for medical imaging. IEEE Trans Med Imag 16(1):96–107

Chowdhury AS, Bhandarkar SM, Robinson RW, Yu JC (2009) Virtual craniofacial reconstruction using computer vision, graph theory and geometric constraints. Patt Recogn Lett 30(10):931–938

Claes P, Vandermeulen D, Greef SD, Willems G, Suetens P (2007) Craniofacial reconstruction using a combined statistical model of face shape and soft tissue depths. Methodology and validation. Forensic Sci Int 159:147–158



Coons SA (1964) Surfaces for computer aided design. Design Division. Mech. Engin. Dept, MIT

Cox MG (1972) The numerical evaluation of B-splines. IMA J Appl Math 10(2):134149

Curry HB, Schoenberg IJ (1947) On spline distributions and their limitsthe polya distribution functions. Bull Am Math Soc 53. Am Math Soc 201 Charles st, Providence, RI 02940-2213, 1114–1114

De Boor C (1978) A practical guide to splines. Math Comput

De Boor C (1972) On calculating with B-splines. J Approx Theory 6(1):5062

De Casteljau P (1959) Outillages mthodes calcul. Andr e Citro en Automobiles SA, Paris

Faux ID, Pratt MJ (1979) Computational geometry for design and manufacture. Ellis Horwood Ltd

Greef SD, Willems G (2005) Three-dimensional craniofacial reconstruction in forensic identification. Latest progress and new tendencies in the 21st century. J Forensic Sci 1(50):12–17

Lee MY, Chang CC, Lin CC, Lo LJ, Chen YR (2002) Custom implant design for patients with cranial defects. IEEE Eng Med Biol Mag 21(2):38–44

Majeed A, Mt Piah AR, Ridzuan Yahya Z (2016) Surface reconstruction from parallel curves with application to parietal bone fracture reconstruction. PLoS One 11(3):e0149921. doi:10.1371/journal.pone.0149921

Majeed A, Mt Piah AR, Gobithaasan RU, Yahya ZR (2015) Craniofacial reconstruction using rational cubic ball curves. PLoS One 10(4):303 e0122854. doi:10.1371/journal.pone.0122854

Majeed A, Piah ARM (2014) Image reconstruction using rational Ball interpolant and genetic algorithm. Appl Math Sci 8(74):3683–3692

Mller A, Krishnan KG, Uhl E, Mast G (2003) The application of rapid prototyping techniques in cranial reconstruction and preoperative planning in neurosurgery. J Craniofac Surg 14:899–914

Ramshaw L (1987) Blossoming: a connect-the-dots approach to splines. Digital Systems Research Center Palo Alto

Sarfraz M, Asim MR, Masood A (2006) A new approach to corner detection, Computer Vision and Graphics. Springer, New York

Sauret V, Linney AD, Richards R (2002) Computer assisted surgery: the use of digital images in enabling computerized design and manufacture of titanium implants. Imaging 14:464–471

Shui W et al (2010) 3D craniofacial reconstruction using reference skull-face database. In: 25th International Conference of Image and Vision Computing New Zealand (IVCNZ). IEEE

Tu P, Book R, Liu X, Krahnstoever N, Adrian C, Williams P (2007) Automatic face recognition from skeletal remains. Proc CVP 07:1–7

Vandermeulen D, Claes P, Loeckx D, Greef SD, Willems G (2006) Paul Suetens Computerized craniofacial reconstruction using CT-derived implicit surface representations. Forensic Sci Int 159S:S164–S174

